INFLUENCE OF THE NUMBER OF BLADES OF THE ARCHIMEDES WIND TURBINE ON ITS PERFORMANCE

IVAN MIHALIK[1], MARIAN LAZAR[1], LUKAS SIMOCKO[1], NATALIA JASMINSKA[1], TOMAS BRESTOVIC[1], ROMANA DOBAKOVA[1]

[1]Department of Energy Engineering, Faculty of Mechanical Engineering, Technical University of Kosice, Kosice, Slovakia

DOI: 10.17973/MMSJ.2024_12_2024043

ivan.mihalik@tuke.sk

Among alternative energy sources, wind energy is one of the fastest growing sectors. However, conventional wind turbines have their limits, especially when it comes to their application in more densely populated areas and in areas with a long-term lower average wind speed. In the future, the Archimedes wind turbine could contribute to an even more significant use of the potential of wind energy. In the present work, four models of Archimedes wind turbines with different numbers of blades were designed and subjected to CFD analysis to determine the power coefficient C_p and torque M_r depending on the tip speed ratio λ. In terms of the achieved torque and the power factor, the 3-blade variant dominated, which compared to the other variants achieved the highest values in almost the entire measured range of the tip-speed ratio.

KEYWORDS

wind energy, Archimedes wind turbine, CFD simulation

1 INTRODUCTION

Wind energy belongs to important renewable energy sources with a high potential for use, and by 2050 it could reach a share of up to 40% of electricity production in Europe. [European Commission 2021]. One of the possibilities of using inexhaustible wind energy is the production of electricity using the Archimedes wind turbine (AWT). The concept of this device was invented in 2003 by Dutch researcher Marinus Mieremet [Owano 2014]. The AWT is one of the small wind turbines, intended mainly as a source of energy for households and smaller social units.

Among the leading features of the device, compared to some types of conventional wind turbines, is the ability to operate even at lower wind speeds and the minimal need for regulation, as the design of the device itself forces the AWT to automatically rotate in the direction of the wind flow [Hameed 2023]. Compared to the Savonius turbine, which can also operate at low speeds and does not require regulation in terms of wind direction, AWT can achieve higher efficiency. The advantage is also low level of the noise, which makes it possible to partially eliminate one of the main disadvantages of using wind energy and thus enable the implementation of AWT in an urban environment as well [Refaie 2021]. The lower risk of bird and bat collisions based on the very design of the turbine is a positive from an environmental point of view.

2 PRINCIPLE OF ARCHIMEDES WIND TURBINE

The operation principle of the AWT is inspired by the so-called Archimedes' screw and consists in the rotating structure of the spiral-type device. Unlike the Archimedes' screw, which was designed to transport fluids and was driven by a crank mechanism, the AWT works on an inverse principle, where the gaseous medium flows around the spirally curved blades of the turbine and sets it in motion. The resulting kinetic and pressure energy is, similarly to conventional wind turbines, transformed into mechanical energy, which is subsequently transferred to an electric generator.

Compared to conventional bladed lift-type wind turbines, such as horizontal axis wind turbine, the AWT is characterized by the fact that it uses not only buoyancy but also pressure force for rotation. The Axial force is represented by vector F_X, while vector F_Y stands for perpendicular force (Fig. 1). The vector C represents the total wind speed, which can be further divided into the circumferential U and relative speed W vectors. The vector W acts perpendicular to the blade wall and the vector U acts perpendicular to the axis of rotation of the turbine. The drag force vector F_D acts parallel to the direction of the vector W, and the lift force vector F_L acts perpendicularly to the drag force vector. By adding these two force vectors, the resultant force R is created [Kamal 2022].

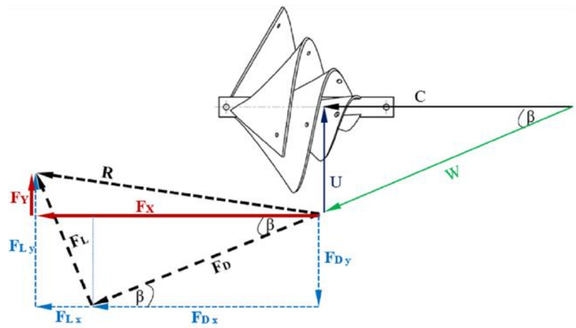

Figure 1. Aerodynamic forces acting on AWT [Kamal 2022]

The AWT rotor is made from a single piece of composite material consisting of plastic and fiberglass. The blades of the turbine, copying the shape of the Archimedean spiral, emerge from the base in the shape of a cylinder. Transverse steel reinforcements prevent the occurrence of vibrations and mutual oscillation of the blades.

3 DETERMINATION OF THE TIP-SPEED RATIO DEPENDENCE ON THE TURBINE REVOLUTIONS

The analysis is devoted to the comparison of the power coefficient against the tip-speed ratio. Tip-speed ratio of the turbine λ can be defined by equation (1) as the ratio of the peripheral speed of the turbine to the speed of the flowing air:

$$\lambda = \frac{v_p}{v_w} \quad (1)$$

where v_p is the peripheral speed of the turbine (m·s^{-1}), v_w – wind speed (m·s^{-1}).

The simulations were carried out using the tip-speed ratio in the range $\lambda \in (0.5; 2.5)$ in five points of this range. The revolutions corresponding to the individual tip-speed ratios can be determined based on the data on the diameter of the turbine and the wind speed after adjusting the equation for calculating the peripheral speed of the turbine:

$$v_p = \omega \cdot \frac{D}{2} = 2\pi \cdot n \cdot \frac{D}{2} = \pi \cdot n \cdot D \quad (2)$$

$$n = \frac{v_p}{\pi \cdot D} \quad (3)$$

where ω is the angular velocity of the turbine (rad·s^{-1}), D – diameter of the turbine (m), n – turbine revolutions (s^{-1}).

By combining equations (1) and (3), it is possible to determine the turbine revolutions at different values of the tip-speed ratio:

$$n = \frac{v_w \cdot \lambda}{\pi \cdot D} \quad (4)$$

Turbine revolutions n after substituting individual values into relation (4) are shown in Tab. 1, considering the wind speed v_w = 5 m·s^{-1} and the turbine diameter D = 0.25 m.

λ (–)	0.5	1	1.5	2	2.5
n (s^{-1})	3.2	6.4	9.5	12.7	15.9

Table 1. Revolutions *n* of AWT depending on the tip-speed ratio *λ*

4 DESIGN OF COMPARED MODELS WITH DIFFERENT NUMBER OF BLADES

The main parameter in the evaluation of the optimal geometry was the number of turbine blades. From the available AWT models implemented in previous research, it can be concluded that the most widespread variant is the configuration with three blades [Mustafa 2020, Nawar 2021, Kamal 2022, Ji 2016, Kim 2014, Patil 2018, Hameed 2023].

Mustafa and Jaleel [2020] compared performance of 3-blade AWT and propeller turbine with wind attack angle effect. Based on experimental measurements in the open stream field, they found that the AWT was more efficient than a propeller wind turbine with comparable parameters for the purposes of electricity production. Nawar et al. [2021] and Kamal et al. [2022] numerically and experimentally investigated the effect of blade design on AWT performance. A detailed comparison of the results demonstrates the higher performance of the variable-angle design over the fixed-angle one. Ji et al. [2016] investigated the effect of the wind direction on the near wake structures of an AWT blade. It has been found that the trajectory of tip vortices varies significantly in the front side plane compared to that of the lee side plane when the angle of attack is higher than 10°. The distance between two consecutive vortices in the front plane decreases monotonically with increasing attack angle, while that in the lee side shows an opposite manner. Kim et al. [2014] investigated aerodynamic characteristics and performance of the designed AWT using CFD simulations. Simulations showed that AWT produced a power coefficient (C_p) of approximately 0.25, which is relatively high compared to conventional types of urban-usage wind turbines. 2D particle image velocimetry (PIV) method in the near field of the blade was used to validate the results using a scale-model. Study of Patil et al. [2018] showed that minimum wind velocity required to function of a 3-blade AWT is 5 m·s^{-1}, however, the optimum wind velocity lies in the interval 18 to 25 m·s^{-1}. Hameed et al. [2023] solved shape optimization of a shrouded AWT for small-scale applications. The results show that the optimal shrouded AWT introduces a maximum C_p 2.58 times higher than value of the bare AWT (C_p = 0.195) at λ = 2.5.

Four AWT models in 2- to 5-blade configurations were designed for analysis purposes. The blades of individual models were distributed around the rotor axis at equal angular spacing according to Tab. 2:

Number of blades (–)	2	3	4	5
Angular spacing (°)	180	120	90	72

Table 2. Angular spacing of blades depending on their number

Fig. 2 shows individual variants of AWT with different number of blades.

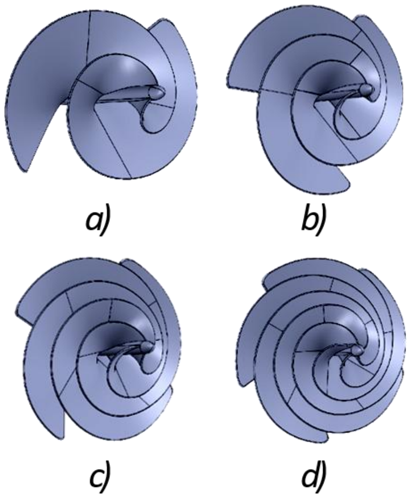

Figure 2. Individual variants according to the number of blades:
a) 2-blade AWT, b) 3-blade AWT, c) 4-blade AWT, d) 5-blade AWT

Fig. 3 and Fig. 4 show the basic design parameters of the 3-blade AWT, while these parameters were the same for the remaining variants. In all variants, the angle of inclination of the blades of all three stages of the turbine was also defined by a value of 60°.

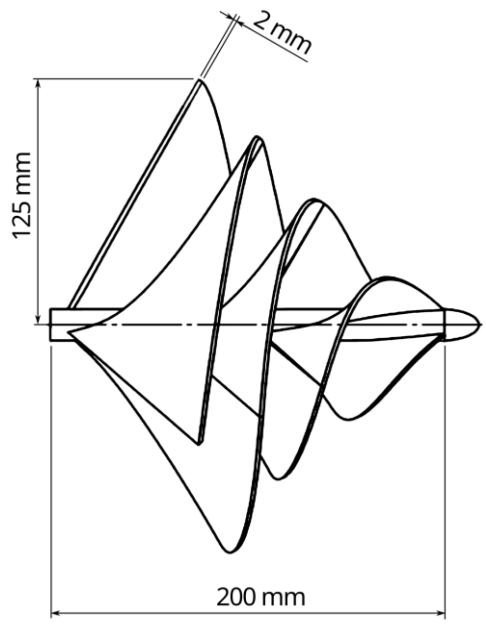

Figure 3. Design parameters of 3-blade AWT

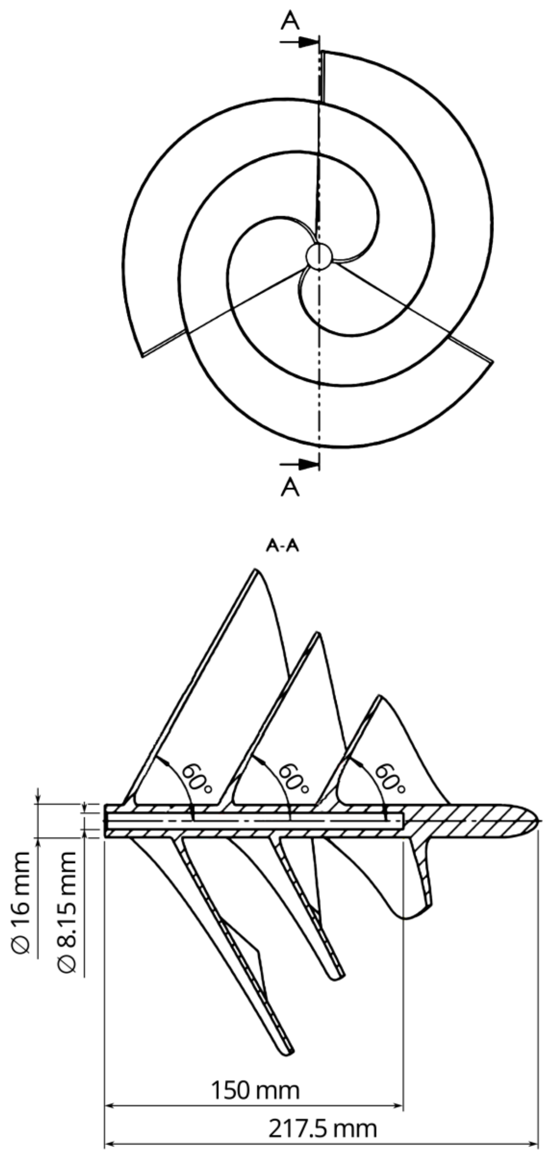

Figure 4. Section of the AWT showing the pitch angle of the blades

The main output parameter of the simulation was the torque in the axis of rotation of the turbine. The values of the torques at the specified revolutions and wind speed of 5 m·s^{-1} are shown in Tab. 3.

Rev. (s^{-1})	M_r (N·m)			
	2 blades	3 blades	4 blades	5 blades
3.2	0.01697	0.02036	0.01880	0.01776
6.4	0.01596	0.01785	0.01677	0.01573
9.5	0.01498	0.01542	0.01464	0.01360
12.7	0.01259	0.01278	0.01195	0.01083
15.9	0.01011	0.00993	0.00889	0.00763

Table 3. Torque depending on the number of blades

Fig. 5 graphically shows the course of the torque depending on the tip-speed ratio for 2- to 5-blade AWTs. It can be observed on the graph that for all variants, except for 2-blade AWT, there is an almost linear regression. The 2-blade variant maintained an almost constant torque in the range of $\lambda \in (0.5; 1.5)$ with increasing revolutions, although at the level of $\lambda = 2$ the curve began to behave similarly to the remaining variants.

It is also clear from Fig. 5 that the 3-blade variant dominates among the other AWT versions, which has the highest torque, except for the area of $\lambda \geq 2.3$. In the second position, there is the 4-blade variant, which maintained the second highest torque up to the point of $\lambda \geq 1.4$. In terms of torque, the already mentioned 2-blade variant is in third place. It surpassed the 5-blade variant at approximately $\lambda \geq 0.95$ and subsequently lost less power than all other variants with increasing revolutions. The 5-blade variant maintained a linear regression, achieving the lowest torque values in 75% of the measured range, placing it last.

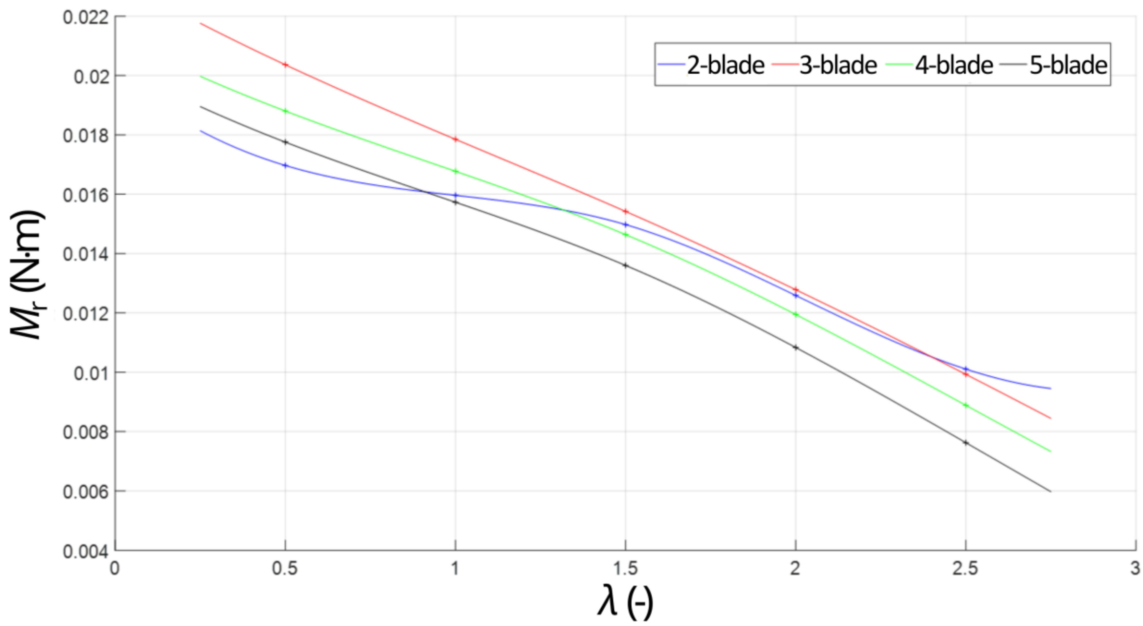

Figure 5. Dependence of the torque M_r on the tip-speed ratio λ

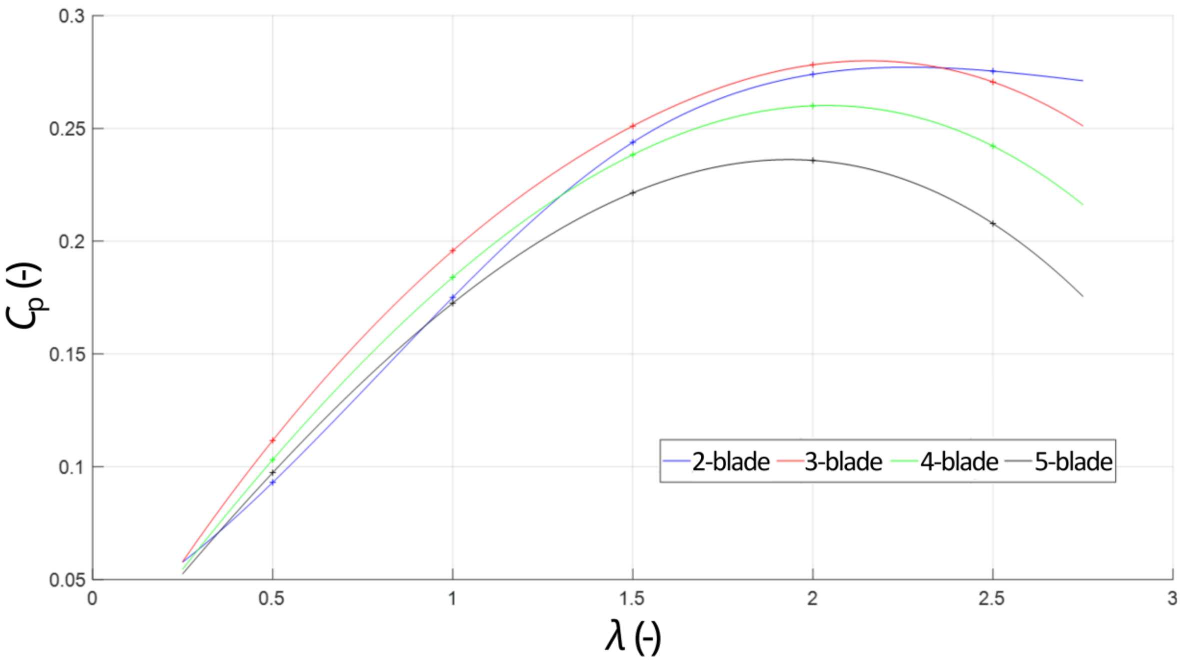

Figure 6. Dependance of the power coefficient C_p on the tip-speed ratio λ

5 DISCUSSION

The power coefficient practically determines the efficiency of the turbine, as it expresses the share of wind energy converted by the turbine into mechanical energy. Its maximum value is $C_{p,max}$ = 0.593, referred to as the Betz limit. Higher efficiencies are not achievable due to the physical nature of air flow. If the turbine could theoretically convert 100% of the energy of the flowing air, it would completely stop the flow of air behind the turbine. In such a case, air would accumulate behind the turbine, which would result in the gradual stopping of the entire column of flowing air and the turbine would not be able to continue operating.

To determine the power coefficient, it is necessary to obtain the corresponding values of the angular velocity ω. With known values of ω and torque M_r, the aerodynamic power of the turbine was calculated:

$$P_{\mathrm{ad}} = M_k \cdot \omega \quad (5)$$

where P_{ad} is aerodynamic power of the turbine (W).

Power coefficient C_p can be calculated using the following equation [Klenovcanova 2006]:

$$C_{\mathrm{p}} = \frac{2 \cdot P_{\mathrm{ad}}}{\rho \cdot A \cdot v_{\mathrm{w}}^3} \quad (6)$$

where ρ is air density at standard conditions (kg·m^{-3}), A – circular surface with the diameter of the turbine (m^2).

The numerically obtained range of the power coefficient in the interval 0.093 to 0.278 correlates with the results achieved in similar research [Nawar 2021, Kamal 2022]. Looking at Fig. 6, it is possible to note a stable increase in the power coefficient in the range of $\lambda \in (0.5;\ 1.0)$. The 3-blade AWT achieved the highest efficiency in this section, followed by the 4-blade AWT. The 5-blade AWT took the third place with a small margin ahead of the 2-blade AWT. However, at the point of approximately λ = 1, the 2-blade AWT already showed a higher efficiency compared to the 5-blade variant. On the interval $\lambda \in (1.0;\ 2.5)$, a gradually increasing difference between the curves of the power coefficient became apparent, with the exception of the 2-blade variant. The growth trend of the C_p curve of the 2-blade turbine had a sharper character, where at λ = 1.5 the 2-blade AWT reached a higher value than the C_p curve of the 4-blade turbine. At approximately the level of λ = 2.3, the 2-blade variant became the most effective with the maximum value of C_p = 0.2754 at the point of λ = 2.5. The overall highest power coefficient C_p = 0.2782 in the measured range was achieved by the 3-blade turbine at the point λ = 2.0. In addition to the highest measured efficiency, up to the point λ = 2.3, the 3-blade AWT also maintained the highest efficiency of all variants.

The 2-blade turbine has the smallest ratio of the actual projection area A_r to the circular area A in the plane perpendicular to the flowing air, but it also has the smallest friction surface of the blades. As the number of blades increases, the actual area of the projection of the turbine A_r also increases (Fig. 7), the friction surface of the blades increases radically while the inter-blade distance decreases. This has the effect that the increase in the number of blades from 2 to 3 increases the performance coefficient C_p. With a further increase in the number of blades, the increase in the area of the turbine projection is negligible compared to the increasing shear surface of the blades. This caused a gradual decrease in the power coefficient for the 4 and 5 blade turbine.

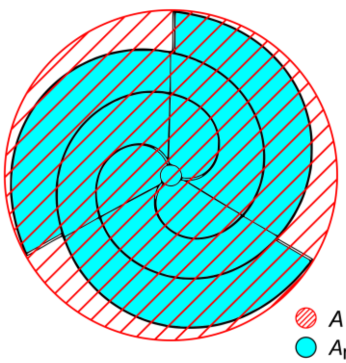

Figure 7. Comparison of an actual projection area A_r and circular area A.

From the point of view of the overall results achieved, the comparison of the 3-blade and 2-blade variant of the turbine is particularly interesting. While the 4-blade and 5-blade AWTs achieved clearly worse results in both analyzes compared to the 3-blade AWT in the entire measured range of the tip-speed ratio, the 2-blade variant of the turbine showed optimal results in the area of the highest measured values of the tip-speed ratio.

6 CONCLUSIONS

In summary, it can be concluded that the 3-blade AWT variant achieved the best overall results both in terms of the achieved power coefficient and torque. The difference in torque indicates a better ability of the turbine to convert wind energy into mechanical energy to rotate the shaft.

The analysis carried out confirmed the global trend in the field of AWT research, which clearly favors the 3-blade variant of the turbine over other options. Despite this fact, and despite that many studies were devoted to the design and construction parameters of AWTs, at the time of writing, the authors have not found any study dealing with the effect of the number of blades on AWT performance. The results obtained through the presented numerical analysis in the Ansys CFX program also provide a basis for future experimental research.

ACKNOWLEDGMENTS

This paper was written with financial support from the VEGA granting agency within the projects no. 1/0224/23 and no. 1/0532/22 and from the KEGA granting agency within the project no. 012TUKE-4/2022.

REFERENCES

[European Commission 2021] Capros, P. et al. EU reference scenario 2020 – Energy, transport and GHG emissions – Trends to 2050. Publications Office, 2021.

[Hameed 2023] Hameed, H.S.A. et al. Shape optimization of a shrouded Archimedean-spiral type wind turbine for small-scale applications. Energy, January 2023, Vol.263, Part B, 125809. ISSN 0360-5442

[Ji 2016] Ji, H.S. et al. Effect of the wind direction on the near wake structures of an Archimedes spiral wind turbine blade. Journal of Visualization, March 2016, Vol.19, pp. 653-665

[Kamal 2022] Kamal, A.M. et al. Blade design effect on Archimedes Spiral Wind Turbine performance: Experimental and numerical evaluations. Energy, July 2022, Vol.250, 123892. ISSN 0360-5442

[Kim 2014] Kim, K.CH. et al. Experimental and Numerical Study of the Aerodynamic Characteristics of an Archimedes Spiral Wind Turbine Blade. Energies, November 2014, Vol.7, No.12, pp. 7893-7914

[Klenovcanova 2006] Klenovcanova, A. and Imris, I. Energy sources and transformations (in Slovak). Kosice, 2006. ISBN 80-89040-29-2

[Mustafa 2020] Mustafa, A.T. and Jaleel, H.A. A comparison study between Archimedes spiral turbine and propeller turbine with wind attack angle effect. AIP Conference Proceedings, March 2020, Vol.2213, No.1, 020058. ISSN 1551-7616

[Nawar 2021] Nawar, M.A.A. et al. Experimental and numerical investigations of the blade design effect on Archimedes Spiral Wind Turbine performance. Energy, May 2021, Vol.223, 120051, ISSN 0360-5442

[Owano 2014] Owano, N. Dutch company launches new-generation urban wind turbines. Techxplore, 2014 [online]. May 2014 [cit. 20.06.2024]. Available from <https://techxplore.com/news/2014-05-dutch-company-new-generation-urban-turbines.html#google_vignette>

[Patil 2018] Patil, Y. Design, Fabrication and Analysis of Fibonacci Spiral Horizontal Axis Wind Turbine. International Journal of Aerospace and Mechanical Engineering, January 2018, Vol.5, No.1, ISSN 2393-8609

[Refaie 2021] Refaie, A.G., Qualitative and quantitative assessments of an Archimedes Spiral Wind Turbine performance augmented by A concentrator. Energy, September 2021, Vol.231, 121128, ISSN 0360-5442

CONTACTS:

Ing. Ivan Mihalik
Technical University of Kosice, Faculty of Mechanical Engineering, Department of Energy Engineering
Vysokoskolska 4, Kosice, 042 00, Slovakia
+421 55 602 2451, ivan.mihalik@tuke.sk